Received: 17 December 2018 | Revised: 17 April 2019 | Accepted: 18 April 2019

DOI: 10.1002/mrm.27808

FULL PAPER

Magnetic Resonance in Medicine

A combined 32-channel receive-loops/8-channel transmit-dipoles coil array for whole-brain MR imaging at 7T

Jérémie Clément[1] | **Rolf Gruetter**[1,2,3] | **Özlem Ipek**[4,5]

[1]LIFMET, Ecole Polytechnique Fédérale de Lausanne (EPFL), Lausanne, Switzerland

[2]Department of Radiology, University of Geneva, Geneva, Switzerland

[3]Department of Radiology, University of Lausanne, Lausanne, Switzerland

[4]CIBM-AIT, Ecole Polytechnique Fédérale de Lausanne (EPFL), Lausanne, Switzerland

[5]School of Biomedical Engineering & Imaging, King's College London, London, United Kingdom

Correspondence
Jérémie Clément, EPFL SB IPHYS LIFMET, Station 6, 1015 Lausanne, Switzerland.
Email:jeremie.clement@alumni.epfl.ch
Twitter: @jeremclem

Purpose: Multichannel receive arrays provide high SNR and parallel-imaging capabilities, while transmit-only dipole arrays have been shown to achieve a large coverage of the whole-brain including the cerebellum. The aim of this study was to develop and characterize the performances of a 32-channel receive-only loop array combined with an 8-channel dipole coil array at 7T for the first time.

Methods: The 8Tx-dipoles/32Rx-loops coil array was characterized by the SNR, g-factors, noise correlation matrix, accelerated image quality, and B_1^+ maps, and compared with a commercial 1Tx-birdcage/32Rx-loops array. Simulated and measured B_1^+ maps were shown for the 8Tx-dipoles/32Rx-loops coil array and compared with the 8Tx/Rx dipole array.

Results: The in-house built 32-channel receive coil demonstrated a large longitudinal coverage of the brain, particularly the upper neck area. G-factors and accelerated MR acquisitions demonstrated robust performances up to $R = 4$ in 2D, and $R = 8$ (4×2) in 3D. A 83% increase in SNR was measured over the cerebellum with the in-house built 8Tx/32Rx coil array compared to the commercial 1Tx/32Rx, while similar performances were obtained in the cerebral cortex.

Conclusions: The combined 32-channel receive/8-channel transmit coil array demonstrated high transmit-receive performances compared to the commercial receive array at 7T, notably in the cerebellum. We conclude that in combination with parallel transmit capabilities, this coil is particularly suitable for whole-brain MR studies at 7T.

KEYWORDS

32-channel, parallel imaging, phased array, SNR, transmit dipoles, ultra-high field

1 | INTRODUCTION

Parallel imaging was originally proposed as a method to combine the high signal-to-noise ratio (SNR) achieved by small surface coils with the large field-of-view (FOV) offered by volume coils.[1] Indeed, in clinical routine (at 1.5T and 3T), the large body volume coils used for the transmit radio frequency (RF) signal generally lack receive sensitivity

and acceleration capability. The simultaneous acquisition of spatial harmonics (SMASH)[2] method made use of the subsequent multiple-receiver signals to enable accelerated image encoding without compromising the SNR. It was followed by the sensitivity encoding (SENSE),[3] and later the generalized auto-calibrating partially parallel acquisitions (GRAPPA)[4] methods, making parallel imaging an important tool for MR applications.[5] However, the accelerated-reconstruction quality is closely related, for example, in SENSE to a clear discrimination between the individual profiles of the receive array elements. Therefore, an efficient spatial decoupling is advantageous between the individual receive elements. Two main methods, coil overlapping and preamplifier decoupling are therefore used when building receive arrays. To characterize the noise amplification associated with increasing acceleration rates, g-factor and noise correlation matrix have been defined.[3] Most of the receive arrays consist of 32 channels,[6-9] but 64-channel[10-12] or even 96-channel[13] arrays have been reported at 3T and 7T, and have shown an increase in peripheral SNR and increased acceleration capabilities.

While receive arrays are widely used at 1.5T and 3T, there are distinct advantages in applying parallel imaging at ultra-high fields (⩾7T), as the SNR increases with the field strength and the number of coils elements.[1,14,15] Therefore, higher spectral[16] and spatial resolutions[17] are achieved. However, there are no available full-body coils at ultra-high field since RF homogeneity is compromised by the shorter wavelength.[18] Receive arrays are therefore built within local transmit coils, typically birdcage or transverse electromagnetic (TEM) coils[19-22] which must be deactivated during receive to avoid interactions between the 2 coils.[23,24] However, they demonstrate at ultra-high field a central brightening effect and low transmit field (B_1^+) is commonly observed in the temporal lobes of the brain.[18,25]

Arrays of multiple independent RF coils have been proposed to improve the B_1^+-field through parallel transmit methods.[26] By manipulating the RF phases and amplitudes[27] of each transmit element in the array, constructive B_1^+-field interferences can be generated over the region-of-interest (ROI) and thus improve the homogeneity of the transmit field. For body imaging, dipole antennas demonstrated an advantageous RF signal penetration depth compared to loop coils[28-30] and were therefore used in transmit array configurations.[31-34] For brain imaging, the extended longitudinal FOV attained with dipoles enables a complete coverage of the brain, including the cerebellum.[35,36] However, only 8-16 transmit channels are usually available, depending on the RF hardware in the scanner. The SNR levels and parallel imaging capabilities being restrained by this limitation, high-density receive-only arrays are used to significantly enhance SNR and parallel imaging.

To maximize the signal, receive arrays are usually placed as close as possible to the head while the transmit arrays surrounding them have a large diameter,[37,38] because of structural constraints. The constrained space of head-gradient 7T MR systems make the construction of combined (transmit/receive arrays separately) designs highly challenging. Nevertheless, the fine adjustment of the geometry can limit strong interactions between the closely placed arrays.[39] A recent approach to increase the number of receivers while maintaining a tight configuration consisted in combining a loop coil array with so-called "vertical loops," resulting in a 16-channel transmit/receive with 16 additional receive-only loop coils.[40] However, while higher SNR was measured at center of the brain, the peripheral SNR was lower compared to a 32-channel receive array without vertical loops.[37,41] Using dipoles, the intrinsic low coupling with loop coils could be exploited as in dipole-loop configuration[42] or in combination with receive-only loop coils, as it was shown for cardiac and spine MRI.[43,44] Nevertheless, while these configurations demonstrated advantageous in-depth receive performances, they were not applied to human brain imaging.

It is advantageous to combine a tight-fitted transmit-only dipole head coil array with a high-density receive-only loop coil array in terms of individual performances of the dipole coil array to cover the whole-brain and of the receive array to improve SNR and acceleration capabilities. However, it is challenging to bring 41-channel RF coils together; combining 7 independent transmit dipoles and 2 quadrature loops with 32 receive-only loop coils in tight fitting configuration around the human head. Moreover, it is still undetermined how the high-density receive-only array would alter the transmit performances of the dipoles. The aim of the present study was, therefore, to design, built and evaluate a 32-channel receive-only loop coil array combined with a tight-fitted dipole head coil array at 7T.

2 | METHODS

2.1 | Receive array

The receive coils were arranged on a 3D-printed (EOSINT P395, EOS, Germany) nylon-helmet (EOS, PA2200) designed to accommodate most of the human heads.[45] The maximal dimension in anterior-posterior direction was equal to 222 mm, of 187 mm from left to right and 231 mm in head-foot direction. The 32 receive loop coils were built with silver plated copper wire, and arranged symmetrically in the left-right direction. To achieve decoupling, neighboring loops were overlapped by approximately 10 mm. Most of the loops were rectangular with their dimensions adjusted according to their position regarding to the transmit array, as each symmetric pairs of dipoles (1 and 6, 2 and 5, 3 and 4) had different lengths, and longitudinal alignment along z-direction. The larger loop coil measured 88 × 60 mm2, and the smaller one 68 × 30 mm2. Three to four loops were positioned under each dipole with their center aligned with the center-line of

the dipoles. To complete the helmet's covering, a few non-rectangular loops were built and placed in-between the others receivers. Particularly, 2 loops were mounted over the subject's eyes without compromising the visual field.

Non-magnetic fixed-value capacitors (American Technical Ceramics, NY, USA) and 2 variable capacitors (Philips Components, Netherlands) were used for tuning/matching of the loops. Each loop was divided symmetrically, and the lumped elements were placed such as none of them would fall under the dipoles' legs. One of the variable capacitors was mounted in parallel of the circuit for impedance matching (Figure 1C, C_M), and was part of the active detuning circuit, including also a PIN diode (MA4P7470F-1072T; M/A-COM, USA) in series with a hand-wounded inductor (Figure 1C, L_1). Together, the capacitor C_M and inductor L_1 formed a parallel resonant circuit tuned at the Larmor

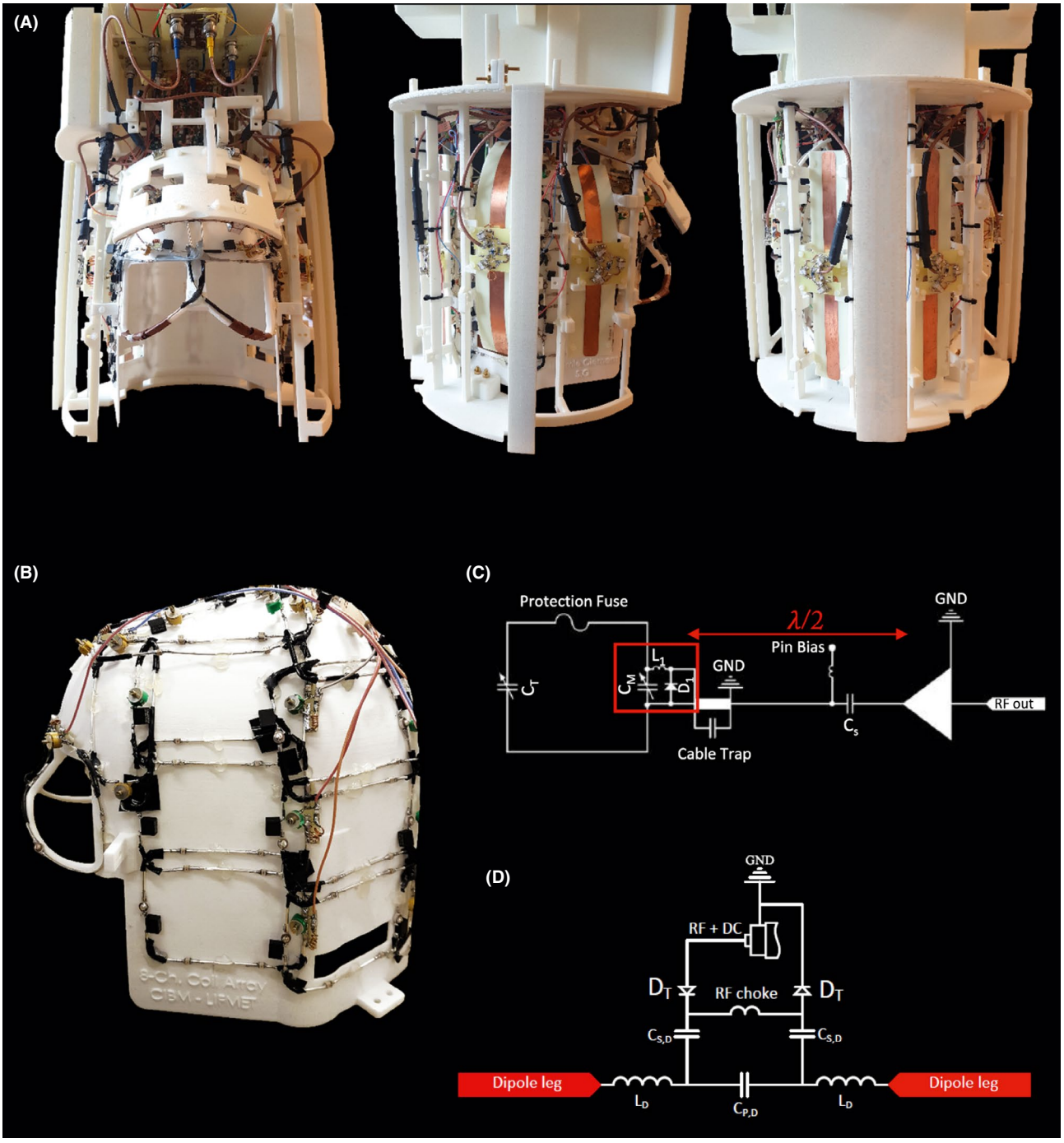

FIGURE 1 A, Photos of the design showing the transmit and the receive arrays B, Photo of the receive array only C, Schematics of a single receive loop circuit. The active detuning circuit is surrounded in red and consists of the PIN diode D_1, the capacitor C_M, and the inductor L_1. D, Schematics of the transmit dipoles showing the active detuning circuit which consisted in the PIN diodes D_T with the RF choke

frequency when the PIN diode is forward biased via the coaxial cable. This DC-enabled trap prevented current from running on the receive loops during transmit. Nevertheless, a protection fuse (400 Series, R ≈ 0.1950 Ω, Littelfuse, USA) was incorporated in series with each loop coil, in case of failure of the active detuning circuit.

The receive coaxial cables (diameter = 1.3 mm, ODU Inc., USA) were routed such as no cable should pass below the dipoles to avoid interactions (Figure 1B). Twelve non-shielded cable traps (1 for 3 cables, and 2 individuals) were added on the path from the loops to the preamplifier board, but placed outside the FOV of the transmit array. Low input impedance preamplifiers (WMM7RP, WanTcom Inc., USA) were used, and preamplifier decoupling was adjusted by making the length of the coaxial cable to be near a half-wavelength (≈34 cm). The low impedance is therefore preserved across the diode D_1 (Figure 1C), which completes the resonant LC circuit (Figure 1C, L_1 and C_M). The subsequent high series impedance introduced, decreases the currents running on the loops, and therefore, reduces the loop coils inductive coupling. All the preamplifiers were placed horizontally on x-z plane and their output was connected to the plugs that fit into the scanner's bed sockets. No additional cable trap was required since the cables from the plugs were positioned largely outside the FOV of the transmit array.

The 32 loop coils ($Q_{unl}/Q_{load} \approx 5.5$ for an isolated receive loop) were tuned and matched on bench using a 4-channel vector network analyzer (Agilent Technologies 5071C-ENA Series, USA) with a head-and-neck phantom loading the coil array, and mimicking the tissues properties of the brain (total volume = 3.850 L of water, 3% of Agar as gelling agent, 9.35 μL/50 mL of Gadolinium and 9 g/L of salt). While the reflection coefficient (S_{11}) of one loop was adjusted, all the other loops were detuned and their respective preamplifier was connected, and powered. To fine-tune the overlap, the coupling values S_{12} were measured for each loop with respect to the neighbor loops, which were connected to the same plug, by replacing the corresponding preamplifiers with a dummy board. The additional isolation provided by preamplifier decoupling was therefore not included. The transmit coil was in-place but detuned via the PIN diodes during all these measurements. To estimate the coupling between the 2 arrays, the S_{12} value was measured between each dipole and the actively-detuned receive loop placed beneath the feeding point of the dipole since it is the most sensitive position in terms of electrical coupling.

A double-pickup probe placed over the receive loops in the array was used to test the active detuning circuit. The S_{12} response curve was measured in the tuned/detuned states to assess the presence of the typical "dip" at Larmor frequency. Similarly, the preamplifier decoupling was tested by comparing the S_{12} response curve with and without the preamplifier in-place.

2.2 | Transmit array

The in-house built transmit coil consisted of 7 center-shortened dipoles and 2 frontal loops in quadrature.[36] Dipoles were etched from 35 μm copper (15 mm width) on a FR4 substrate with a thickness of 0.1 mm, and lengths ranging from 158.5 mm to 230 mm. They were geometrically arranged such as the maximal distance between the dipoles and the helmet was around 15 mm. However, the passive decoupling dipoles were removed from the original design since they could not be detuned, and therefore, interfered with the receive array adjustments. For the transmit dipoles, PIN diodes were added in series of the tuning/matching circuit to actively detune them during the signal's reception, with the DC current coming through the RF cables (Figure 1D). The 2 transmit loops (95 × 85 mm2) were placed over the frontal region. A PIN-diode was added in series with an hand-wounded inductor, and connected in parallel of a capacitor in the loop to enable active detuning during receive mode. Common-modes on the coaxial cables were diminished with a balun that is a quarter-wavelength transformer tuned to 297.2 MHz with capacitors. Tuning/matching to 297.2 MHz and S-parameter matrix measurement were performed using the vector network analyzer.

2.3 | Electromagnetic field simulations

An accurate model of the in-house built 8Tx/32Rx RF coil array was simulated with the finite-difference time-domain (FDTD) method on Sim4Life 4.2 (ZMT AG, Switzerland) on a whole body human model, Duke.[46]

All transmit coil array's elements (dipoles and loops) were defined as perfect electric conductors (PEC), gridded at 3 mm-iso, and with lumped elements according to the realistic coil design. The Duke model was gridded at 2 mm-iso, and truncated below the torso to decrease the total grid size (80 Mcells). All the transmit coils were driven individually by a Gaussian excitation centered at 297.2 MHz with a 500 MHz bandwidth and computations were carried out on a dedicated GPU (1 × GTX 1080Ti, Nvidia Corp., USA) with an average simulation time of 16 hour per channel for 150 periods of excitation to ensure convergence of the simulation. Transmit coils were tuned and matched to 297.2 MHz at 50 Ohms better than −15 dB.

The receive loop coils were modeled as wires, and defined as perfect electric conductors (PEC). To ensure an accurate placement of the loops, the 3D model of the helmet was imported into Sim4Life. Each loop was segmented according to the built model and capacitors (6 pF) and fuses (R ≈ 0.2Ω) were added. The open-circuit condition was satisfied for the active detuning during the transmit. The PIN diodes, receive coaxial cables, and cable traps were not included in the simulation. The total receive array was gridded at 1.2 mm-iso,

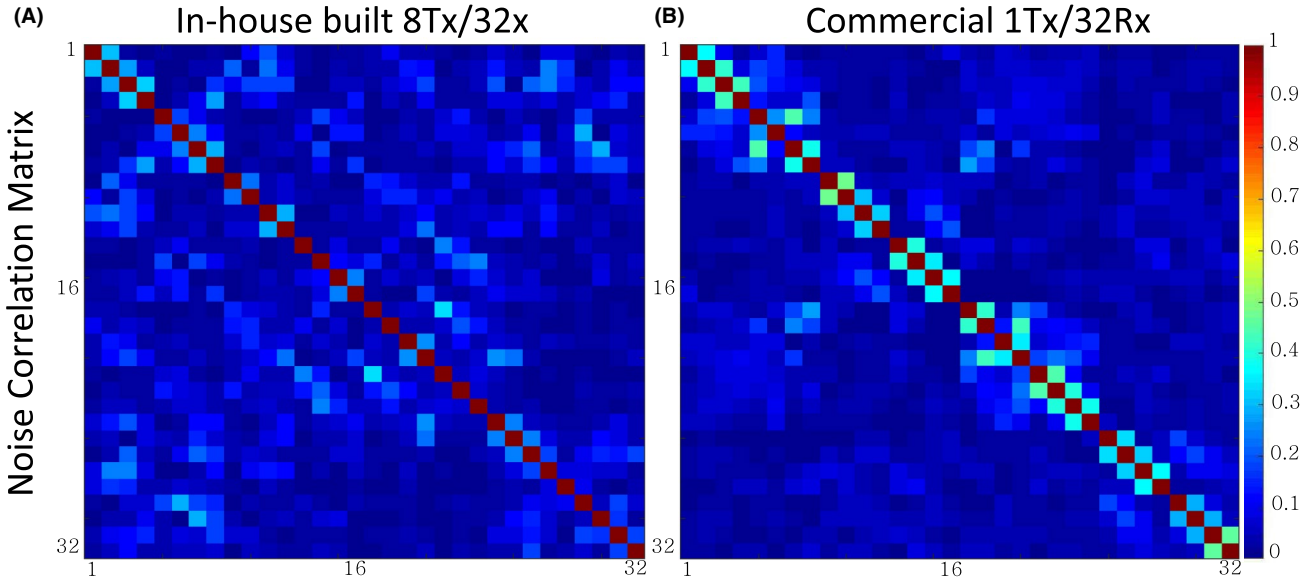

FIGURE 2 Noise correlation matrices calculated for A, the in-house built 8Tx/32Rx coil array (mean = 6%, max = 33%) and B, the commercial 1Tx/32Rx coil (mean = 6%, max = 47%). The diagonal terms were normalized to 1

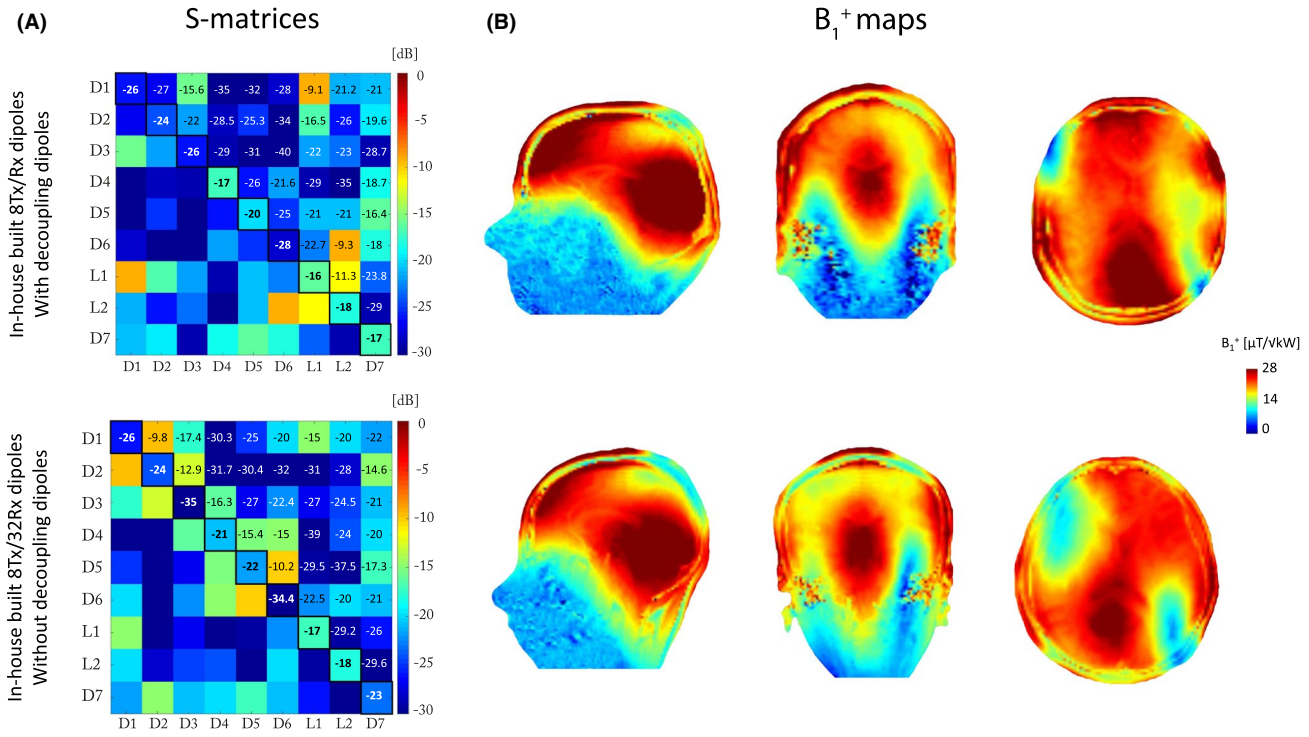

FIGURE 3 For the in-house built 8Tx/Rx coil array with decoupling dipoles (upper row) and the in-house built 8Tx/32Rx coil array without the decoupling dipoles (bottom row): A, Scattering matrices measured on the phantom. B, Experimentally measured RF shimmed B_1^+ maps on the human brain, for RF phases optimized in sagittal slice, and normalized to 1 kW delivered (at the coil plug) peak-power per channel. Two different subjects are shown

and the voxelization was carefully verified such as the loops overlapped without touching each others as in the realistic RF coil array.

The B_1^+ maps were normalized to 1 kW delivered power per channel, and included the transmit losses measured at 37% from the RF amplifiers to the coil plug (Siemens, Erlangen, Germany) and ≈13% from the coil plug to the RF coils. SAR_{10g} maps and 10-gram tissue-averaged Q-matrices[47] were evaluated, and the worst-case local SAR value was used for the MR experiments to ensure the subject's safety.

2.4 | MR experiments

All the measurements were performed on a 7T Magnetom MR scanner equipped with 8 × 1 kW RF amplifier (Step 2.3, Siemens, Erlangen, Germany) and 32 receive channels on healthy volunteers (2 women and 2 men, mean age = 26 years old) who had signed a written consent approved by the local ethics committee. Phase-only RF shimming was performed using a particle-swarm optimization (PSO) method.[48,49]

Two-dimensional (2D) sagittal (head-foot phase encoding) and transverse (anterior-posterior phase encoding) fully sampled GRE images (1 × 1 mm2, slice thickness = 1 mm, TR/TE = 1000/3.37 ms, FA = 48°, 192 × 192 matrix) were acquired with the RF phases optimized according to the slice orientation and areas-of-interest. Receive noise correlation matrix was computed from a noise-only scan (no RF excitation). Receive coil sensitivities were estimated from the raw data by dividing the reconstructed signal from each loop with the sum-of-squares of all the receivers. The image was reconstructed in SNR units for no-acceleration,[50] including the noise covariance information but without B_1^+-correction. The raw data were under-sampled in post-processing by setting to 0 the lines in k-space, according to the acceleration rate needed, and reconstructed with the SENSE method.[3] The g-factor maps were calculated for the whole FOV, and for acceleration factors of 2, 3, 4, and 5 in left-right (LR) direction for the transverse slice and anterior-posterior (AP) in sagittal, to assess the noise amplification during SENSE reconstruction. Three-dimensional (3D) GRE images (1 × 1 × 1 mm3, TR/TE = 8/2.34 ms, FA = 10°, 256 × 256 matrix, AP phase encoding) were acquired to evaluate the acceleration performances in 2 directions. All these results were compared to a commercial single Tx birdcage coil with 32-channel receivers (Nova Medical, USA).

All the B_1^+ maps were acquired with a SA2RAGE sequence for a 500 µs, 90° hard pulse, and normalized to 1 kW peak-power (at the coil plug) per channel.[51] The transmit field maps acquired with the in-house built 8Tx/32Rx coil array were compared to the commercial 1Tx/32Rx coil and to the in-house built 8Tx/8Rx dipole coil array with decoupling dipoles. B_1^+ sensitivities (magnitude and phase) were derived on Matlab from a GRE-based sequence.

2.4.1 | Anatomical images

RF phases of the individual channels were optimized with the PSO method in central sagittal slice and the RF shimmed B_1^+ maps were measured to evaluate the influence of the receivers. MR images were acquired with the 3D turbo-spin echo (3D-TSE, TE/TR = 120/2000 ms, resolution = 0.8 × 0.8 × 0.8 mm3, FOV = 210 × 210 mm2, Turbo Factor = 60,

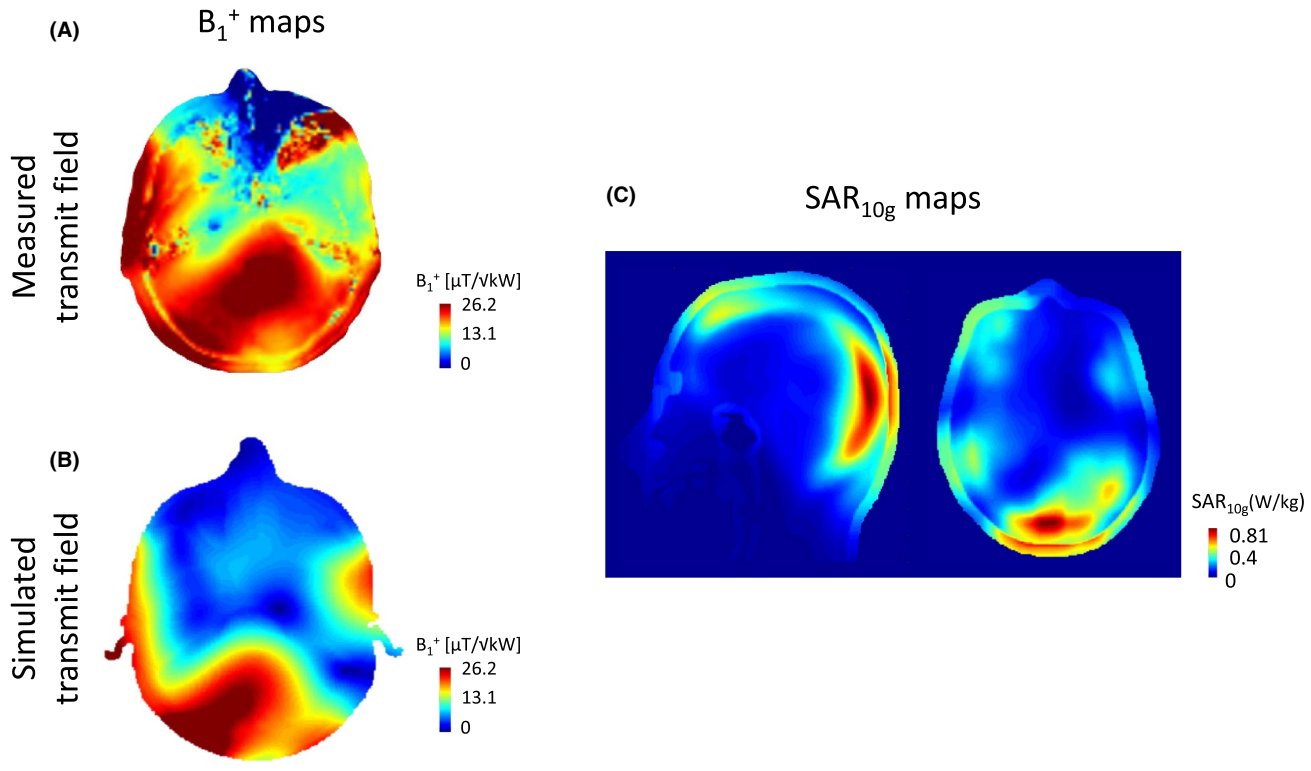

FIGURE 4 For the in-house built 8Tx/32Rx dipole coil array—A, Experimentally measured RF phase-shimmed B_1^+ map for a mid-transverse slice in the cerebellum, and normalized to 1 kW delivered peak-power per channel at the coil plug. B, Corresponding simulated B_1^+ map, normalized to 1 kW delivered (including RF losses) peak-power per channel. C, SAR_{10g} maps computed for the RF phases used in B, and normalized to 1W input power. The sagittal and transverse slices are shown at the position of the maximal SAR_{10g} value, and scaled to this value

GRAPPA = 2, TA = 10 min 25 seconds), MP2RAGE (resolution = 0.6 × 0.6 × 0.6 mm3, FOV = 192 × 192 mm2, Grappa = 3, TA = 10 minutes 04 seconds),[52] and multi-slice GRE (TE/TR = 16/1000 ms, resolution = 0.3 × 0.3 × 3 mm3, FA = 60°, slices = 8, FOV = 210 × 210 mm2, GRAPPA = 4, TA = 2 minutes 58 seconds) sequences.

3 | RESULTS

The in-house built 32-channel receive array achieved –30 dB isolation between the tuned and actively detuned states, and −25 dB difference with and without the preamplifiers connected. With the preamplifiers replaced by a dummy board, a maximal coupling value of −10 dB was measured between the in-house built receive loops whose overlap could not be optimized, because of geometrical constraints. With the preamplifiers in-place, sufficient decoupling was achieved between the 32 loops, with a mean and a maximum noise correlation of 6% and 33%, respectively (Figure 2A). In comparison, the commercial 1Tx/32Rx coil demonstrated a maximum noise correlation of 47%, and a similar mean value (Figure 2B).

When the decoupling dipoles were removed, the dipoles demonstrated an elevated maximum coupling of −9.8 dB compared to the in-house built 8Tx/Rx RF coil array,[36] while all the reflections coefficient were below −15 dB (Figure 3A). High isolation (better than −35 dB) was measured between the transmit dipoles and the actively detuned receive loops located beneath the feeding point. For the frontal transmit loops, a −25 dB isolation was measured with the in-house built receivers. No substantial loss in transmit field efficiency (approximately 7%) was measured over a central axial slice with the in-house built 8Tx/32Rx coil array when the decoupling dipoles were removed and the receivers in-place (Figure 3B). Moreover, while the overall transmit field distribution patterns were comparable, a slight enhancement of the transmit efficiency was measured in the lower brain and the cerebellum areas (Figure 3B). With the commercial 1Tx/32Rx coil array (single-Tx birdcage coil), lower power was required to get a 90° flip angle at center of the brain compared to the in-house built 8Tx/32Rx dipole coil array. However, better B_1^+-field homogeneity was achieved with the in-house built 8Tx/32Rx dipole coil array (Supporting Information Figure S1).

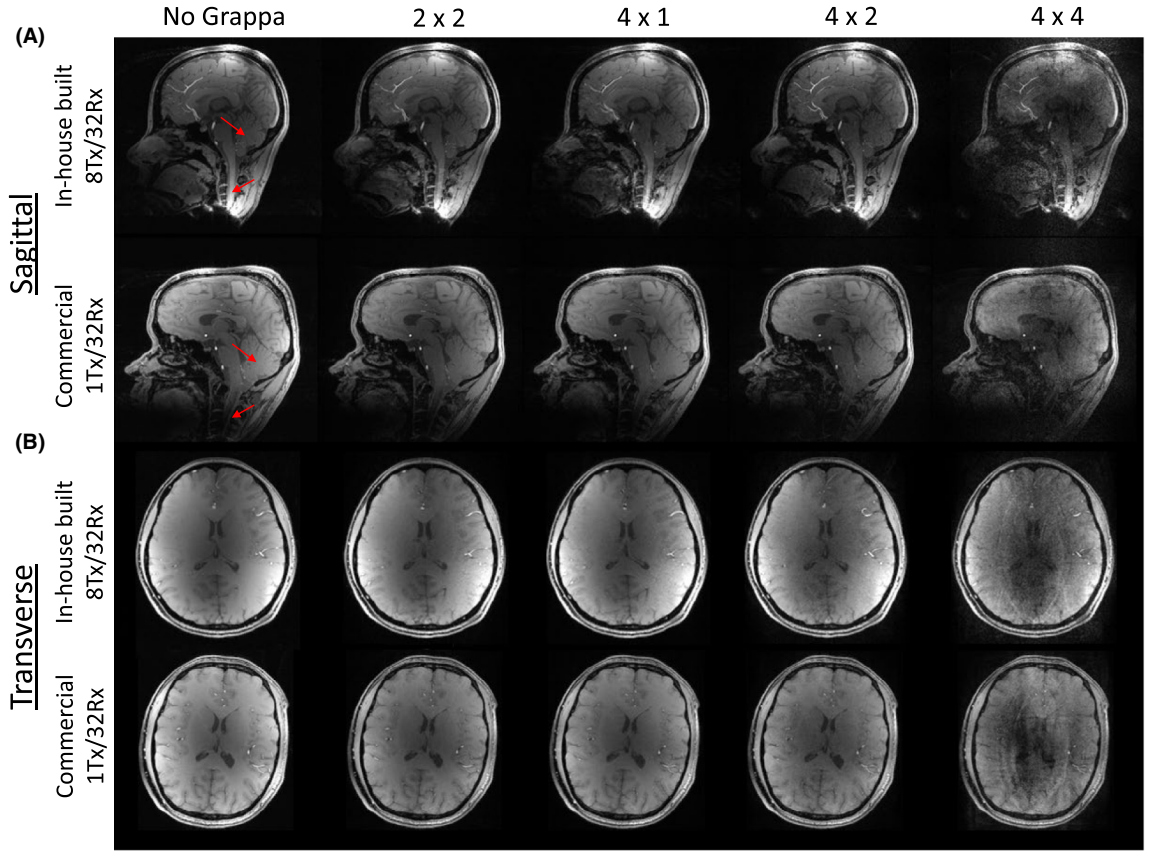

FIGURE 5 3D-GRE images, shown in A, sagittal and B, transverse slices, and acquired at different acceleration factors for the in-house built 8Tx/32Rx coil array and the commercial 1Tx/32Rx coil. The same parameters were used, but 2 volunteers are shown. The red arrows point to the areas where the signal quality was improved for the in-house built 8Tx/32Rx coil compared to the commercial 1Tx/32Rx coil. The scales were adjusted to display comparable intensities

The transmit field map acquired on the human brain for the RF phases optimized over the cerebellum demonstrated similar pattern compared to the simulated result (Figure 4A-B). Even though the reflection coefficients were higher (maximum value of –4 dB), the coupling matrix for the simulated 8Tx/32Rx coil array was comparable to the fabricated RF coil array. The corresponding simulated $SAR_{10g,\,max}$, normalized to 1W input power was 0.81 W/kg and localized at the back of the head (Figure 4C).

The 3D-acquisitions with 8-times (4 × 2) acceleration were without significant alteration of the signal for both the in-house built 8Tx/32Rx coil array and the commercial 1Tx/32Rx coil (Figure 5A). Nevertheless, the cerebellum appeared more blurred in sagittal slices with the commercial 1Tx/32Rx coil since the transmit field was low in this area. In transverse slices, the 2 receive arrays demonstrated similar results with lower signal intensity at the center of the brain (Figure 5B). Both coils produced similar mean g-factor values for an acceleration up to R = 4, while the maximal g-factor value was in most cases lower for the commercial 1Tx/32Rx coil (Figure 6). At R = 5, the mean g-factor for both coils were increased to approximately 1.65 in sagittal, and 1.55 in transverse slices. Multi-slice high-resolution (0.3 mm^2 in-plane) GRE images were acquired at R = 4, and demonstrated an unaltered signal in cerebral cortex and cerebellum for the in-house built 8Tx/32Rx dipole coil array (Figure 7). However, acceleration-related artifacts were observed in the brain stem, where the g-factor values were maximal. The highest SNR values were achieved at the periphery of the brain (Figure 6), as expected when using surface loop coils. Mean SNR values of 115 and 104 were measured over the brain in transverse and sagittal slices with the in-house built 8Tx/32Rx coil array. In comparison, the commercial 1Tx/32Rx coil demonstrated similar values (111 in transverse and 90 in sagittal) (Figure 6). Over the mid-cerebellum (Figure 8), a mean SNR of 121 was measured with the in-house built 8Tx/32Rx coil array, which represents a 83% increase compared to the commercial 1Tx/32Rx (mean SNR of 66).

A high signal homogeneity was observed over the cerebellum in the high-resolution 3D-TSE (0.8 mm^3, Figure 9A) and MP2RAGE images (0.6 mm^3, Figure 9B). Over the whole-brain, the high-resolution (0.6 mm^3) MP2RAGE images demonstrated the large coverage achieved with the in-house built 8Tx/32Rx (Figure 10, see

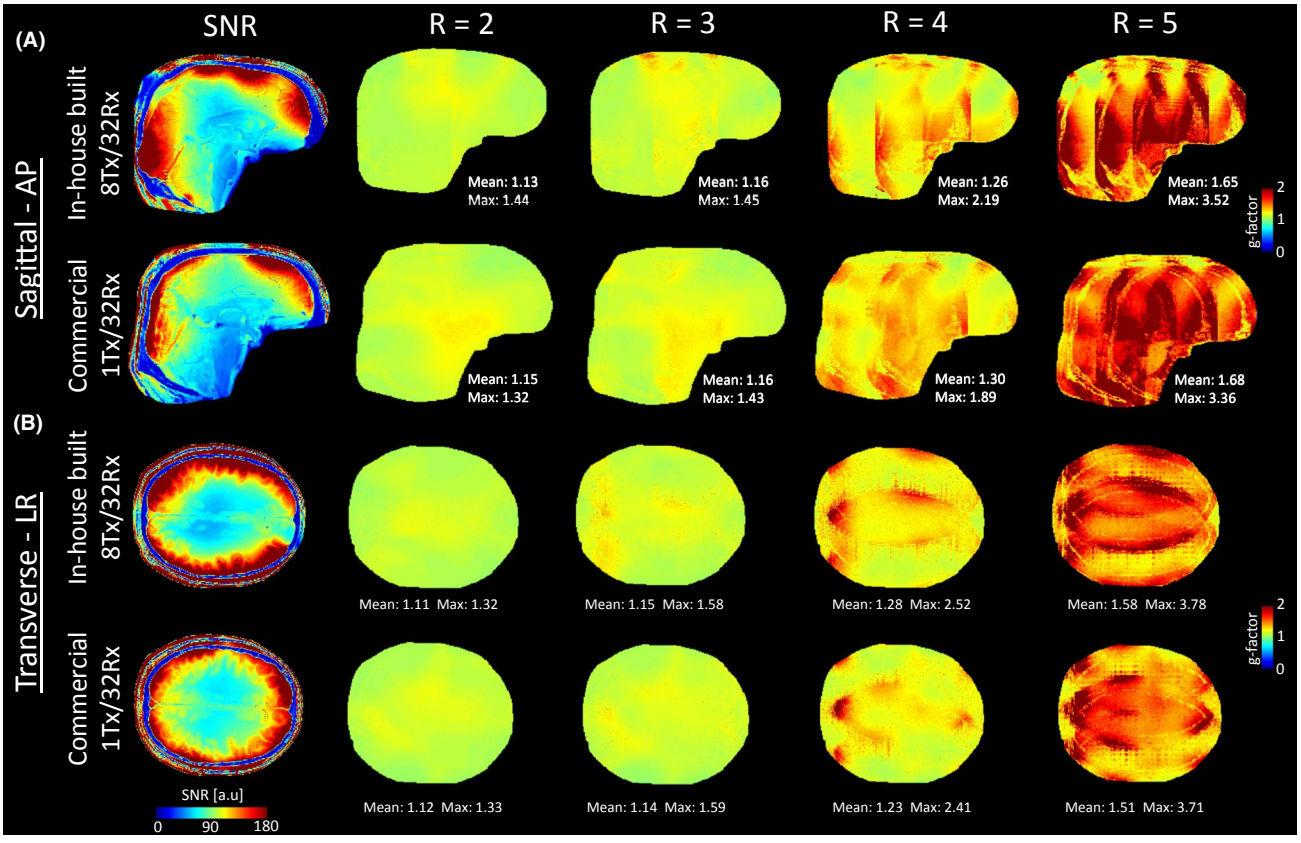

FIGURE 6 SNR and g-factor maps, for the in-house built 8Tx/32Rx coil array and the commercial 1Tx/32Rx coil in A, sagittal (different volunteers with comparable head shape and size) and B, transverse slices. The g-factor maps were computed at $R = 2$, 3, 4, and 5 in anterior-posterior direction for the sagittal slice and in left-right direction for the transverse slice. The RF phases were optimized for A, in the sagittal slice and B, in the transverse slice

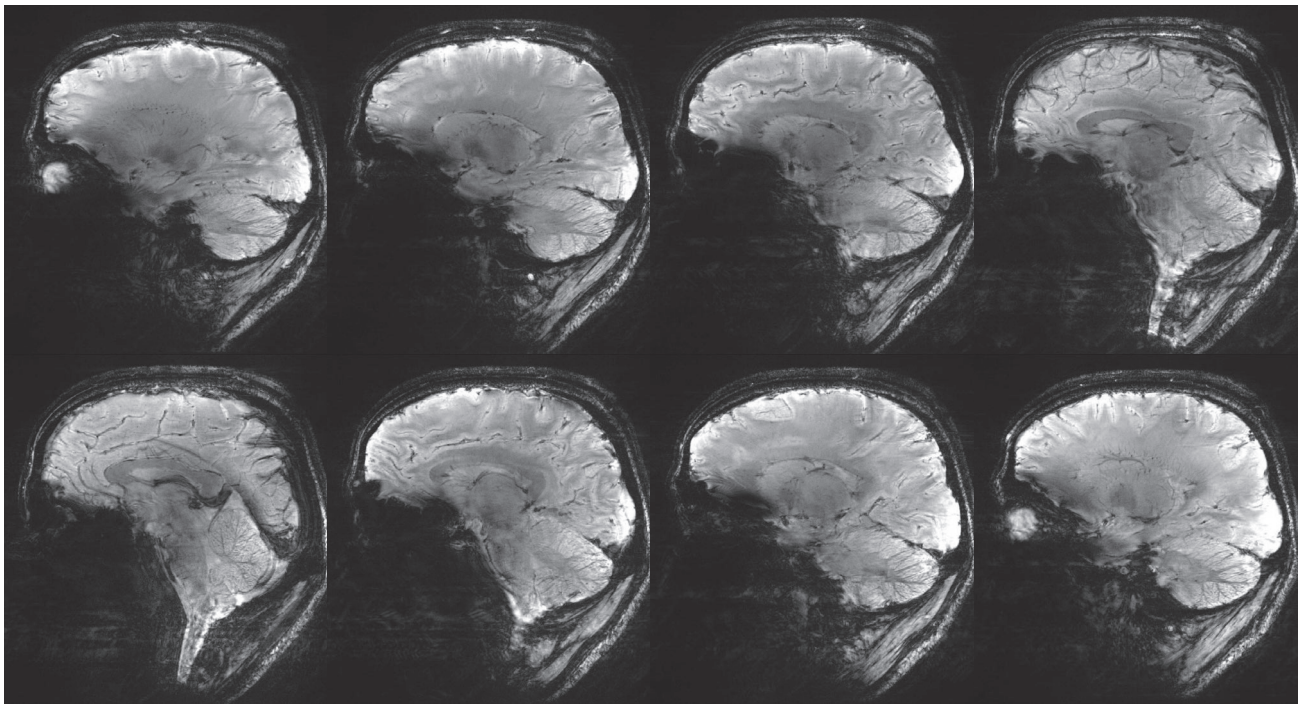

FIGURE 7 High-resolution (0.3 mm2 in-plane) multi-slice GRE images acquired at $R = 4$, shown for the in-house built 8Tx/32Rx coil array. No post-processing correction was applied

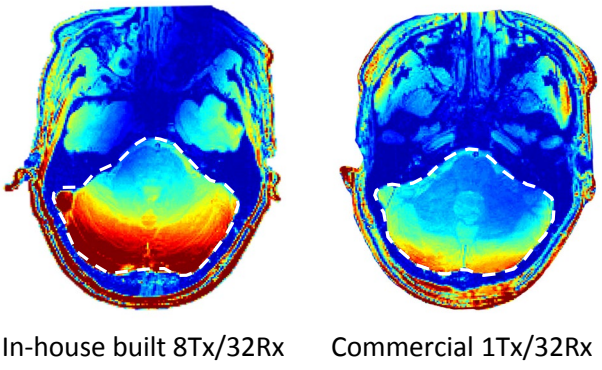

FIGURE 8 Measured SNR maps for the in-house built 8Tx/32Rx coil array and the commercial 1Tx/32Rx coil in mid-cerebellum slice. The mean SNR value was calculated over the white-dashed area, for RF phases optimized in the cerebellum

also Supporting Information Video S1 showing all the slices in sagittal orientation).

4 | DISCUSSION

The present study shows for the first time that significant performance improvements were obtained in low-brain SNR and coverage for the combination of a 32-channel receive array with a tight-fitted dipole transmit coil array. The design exploited the placement of 32 receive loop coils on a helmet designed to minimize the distance with the head.

The placement of 32-channel independent receivers contributed to enhance the signal in low-brain and cerebellar regions. Indeed, while the position of the dipoles was optimized to maximize both the transmit field and coverage of the brain, the multi-receivers could be centered over more local areas. The brain stem was, for example, homogeneously covered with high SNR in the MP2RAGE results (Figure 10). For optimized RF phases in the mid-cerebellum slice, the SNR gain was clearly demonstrated compared to the commercial 1Tx/32Rx coil (Figure 8), which could improve, for example, MR of the cerebellum. The 3D-GRE images demonstrated a well-detailed cerebellum with the in-house built 8Tx/32Rx coil array while the tissue's contrast was altered for the commercial 1Tx/32Rx coil due to the lack of transmit field (Figure 5).

The low-noise correlation coefficients achieved with the in-house built 32-channel receive array demonstrated an efficient decoupling of the loops. However, these values include the additional isolation provided by preamplifier decoupling, and not only the overlap efficiency. The commercial 1Tx/32Rx coil demonstrated in comparison increased noise coefficients between neighbors with a maximal coupling 48% stronger than the in-house built 8Tx/32Rx coil array. Both coils produced nevertheless a similar mean noise correlation value, lower than 32-channel receive arrays previously reported at 7T.[53-55] Signal quality was essentially preserved in accelerated 3D-GRE acquisitions up to $R = 8$ (4×2 in AP direction). A slight increase in SNR was observed at the top of the head and in the occipital lobe with the in-house built

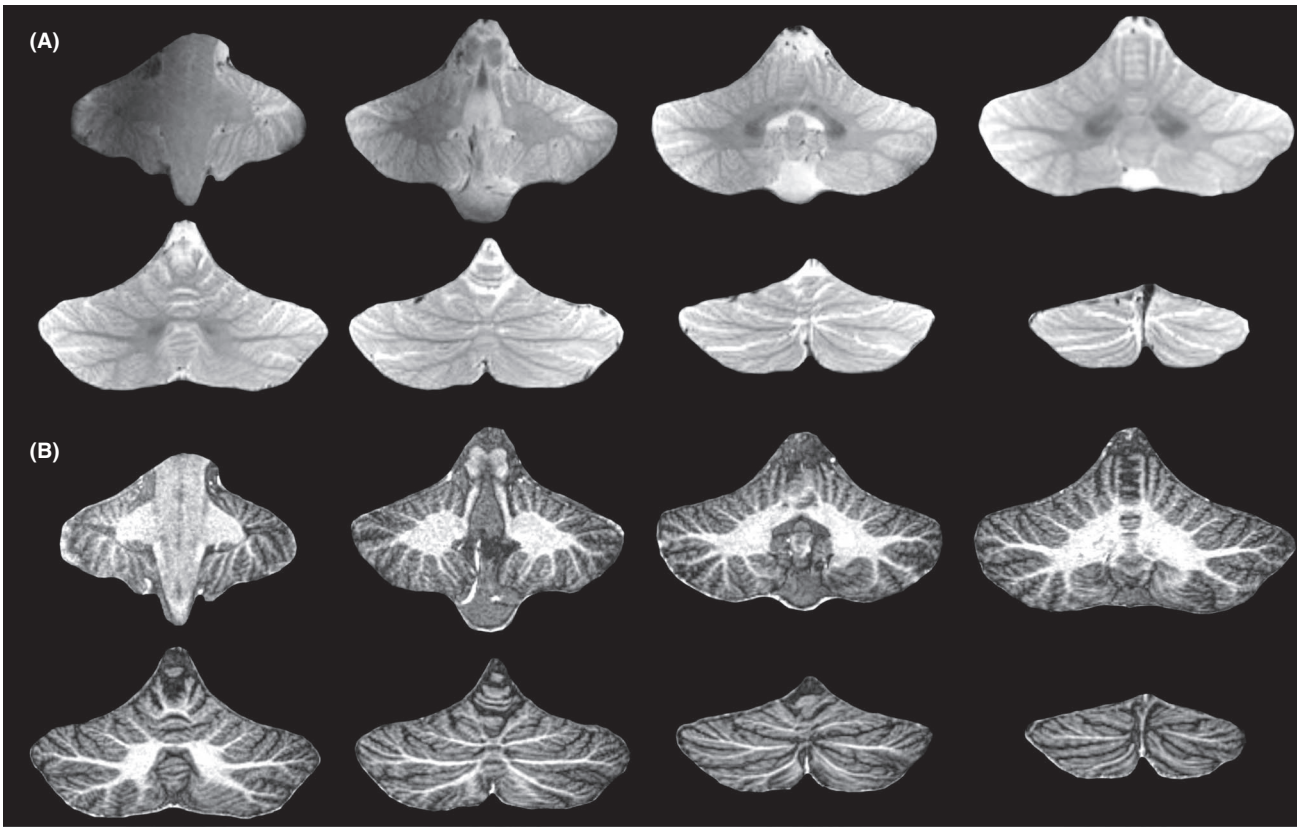

FIGURE 9 For the in-house built 8Tx/32Rx coil array—A, High-resolution 3D TSE images ($0.8 \times 0.8 \times 0.8$ mm3) and MP2RAGE ($0.6 \times 0.6 \times 0.6$ mm3) images of the cerebellum displayed for 8 coronal slices, and for the RF phases applied in Figure 4A. No post-processing correction was applied

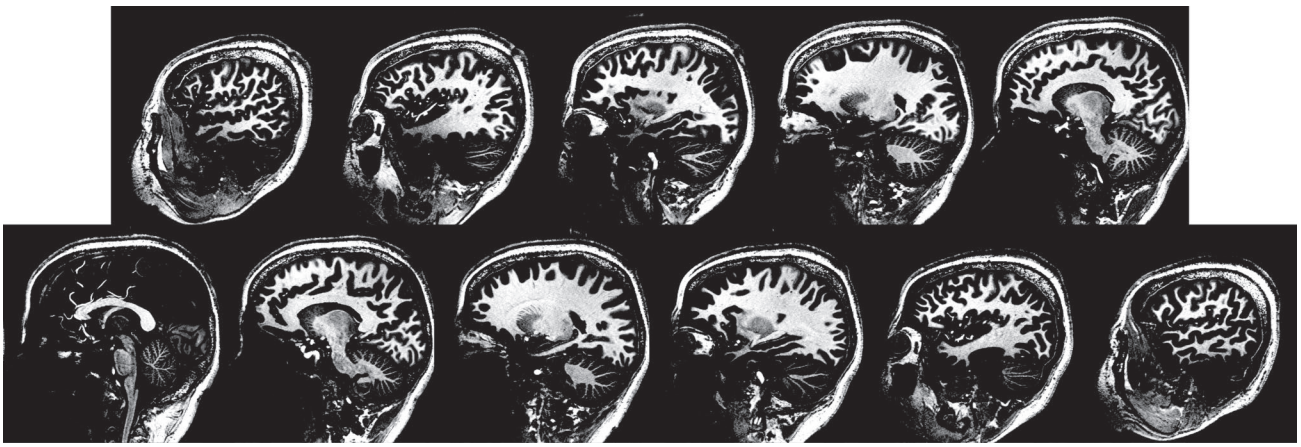

FIGURE 10 High-resolution ($0.6 \times 0.6 \times 0.6$ mm3) MP2RAGE images acquired with the in-house built 8Tx/32Rx coil array, and shown for sagittal slices taken each 9.6 mm, and covering the whole-brain. No post-processing correction was applied [movie is available online as Supporting Information Video S1]

8Tx/32Rx coil compared to the commercial 1Tx/32Rx coil, while comparable SNR value was measured at the middle of the brain. In future developments, the transmit dipoles could be included as combined or multiple receivers since their current distribution pattern was shown to be advantageous for in-depth SNR performances at ultra-high fields.[56] The g-factors appeared to be relatively insensitive to the direction of acceleration, as the mean values were comparable in transverse and sagittal slices. However, in sagittal slice the g-factor achieved with the in-house built 8Tx/32Rx was impaired by a sub-optimal overlap efficiency due to the geometrical constraints of the design. Consequently, higher peak values were measured compared to the commercial 1Tx/32Rx coil at all acceleration rates.

The transmit field distribution was not significantly modified and the B_1^+ efficiency was only slightly decreased (by approximately 7%) compared to the in-house built 8Tx/Rx dipole coil array with decoupling dipoles. Moreover, the modified coupling values between the dipoles when the decoupling method was removed may have contributed to the enhancements observed in the cerebellum. The adequate placement of the receivers and the efficient decoupling between the 2 arrays could be assessed since no shielding effect or transmit field cancellations were observed. It is therefore of utmost importance to carefully align the receive loops with the dipoles such as the active-detuning circuit is distant from the dipole's feeding point when designing equivalent coil arrays. Similarly, no lumped element should be positioned under the dipoles. While the multi-receivers can locally improve the signal quality in low-field areas, larger inhomogeneities may be visible. Phase-only RF shimming being limited to optimize the homogeneity over large regions, other techniques such as the recently-proposed universal pulses, kt-points or spiral non-selective RF pulses could be used.[57-60] The field of applications of the in-house built 8Tx/32Rx coil array could therefore be extended to others MR experiments such as functional MRI.

No significant differences were observed in terms of transmit field intensity and distribution with the simulated 8Tx/32Rx dipole coil array compared to the simulation model not including the receivers. This is consistent with the experimental results. The SAR_{10g} levels calculated e.g for optimized RF phases in the cerebellum were moderate given the high intensity and homogeneity of the transmit field which was achieved.

5 | CONCLUSION

The combined 8-channel dipole coil array with a 32-channel receive-only loop coil array was investigated and demonstrated high transmit/receive properties over the whole-brain. Moreover, the coil dimensions were compatible with head-only MR systems. Parallel imaging and SNR performances were compared to a commercial 1Tx/32Rx coil. While both coils produced comparable SNR at the periphery of the cerebral cortex, the in-house built 8Tx/32Rx coil array demonstrated superior results in the low-brain and cerebellum regions. We conclude that these properties combined to the parallel transmit capabilities make this coil particularly suitable for whole-brain MR studies at 7T.

ACKNOWLEDGEMENTS

This study was supported by Centre d'Imagerie Biomedicale (CIBM) of the UNIL, UNIGE, HUG, CHUV, EPFL, and the Leenaards and Jeantet Foundations.

ORCID

Özlem Ipek https://orcid.org/0000-0001-5233-1600

REFERENCES

1. Roemer P, Edelstein W, Hayes C, Souza S, Mueller O. The NMR phased array. *Magn Reson Med*. 1990;16:192–225.
2. Sodickson DK, Manning WJ. Simultaneous acquisition of spatial harmonics (smash): fast imaging with radiofrequency coil arrays. *Magn Reson Med*. 2005;38:591–603.
3. Pruessmann KP, Weiger M, Scheidegger MB, Boesiger P. Sense: sensitivity encoding for fast MRI. *Magn Reson Med*. 1999;42:952–962.
4. Griswold MA, Jakob PM, Heidemann RM, et al. Generalized autocalibrating partially parallel acquisitions (GRAPPA). *Magn Reson Med*. 2002;47:1202–1210.
5. Adalsteinsson E, Aksoy M, Atkinson D, et al. *Parallel Imaging in Clinical MR Applications*. Berlin Heidelberg New York: Springer; 2007.
6. Wiggins G, Triantafyllou C, Potthast A, Reykowski A, Nittka M, Wald L. 32-channel 3 tesla receive-only phased-array head coil with soccer-ball element geometry. *Magn Reson Med*. 2006;56:216–223.
7. Zhu Y, Hardy CJ, Sodickson DK, et al. Highly parallel volumetric imaging with a 32-element RF coil array. *Magn Reson Med*. 2004;52:869–877.
8. Keil B, Alagappan V, Mareyam A, et al. Size-optimized 32-channel brain arrays for 3 t pediatric imaging. *Magn Reson Med*. 2011;66:1777–1787.
9. Zwart JAD, Ledden PJ, Gelderen PV, Bodurka J, Chu R, Duyn JH. Signal-to-noise ratio and parallel imaging performance of a 16-channel receive-only brain coil array at 3.0 tesla. *Magn Reson Med*. 2004;51:22–26.
10. Keil B, Blau JN, Biber S, et al. A 64-channel 3t array coil for accelerated brain MRI. *Magn Reson Med*. 2012;70:248–258.
11. McDougall MP, Wright SM. 64-channel array coil for single echo acquisition magnetic resonance imaging. *Magn Reson Med*. 2005;54:386–392.
12. Ugurbil K, Auerbach E, Moeller S, et al. Brain imaging with improved acceleration and SNR at 7 Tesla obtained with 64-channel receive array. *Magn Reson Med*. 2019;82:495-509.
13. Wiggins GC, Polimeni JR, Potthast A, Schmitt M, Alagappan V, Wald LL. 96-channel receive-only head coil for 3 tesla: design optimization and evaluation. *Magn Reson Med*. 2009;62:754–762.
14. Hoult D, Richards R. The signal-to-noise ratio of the nuclear magnetic resonance experiment. *J Magn Reson*. 2011;213:329–343. Magnetic Moments.
15. Vaughan J, Garwood M, Collins C, et al. 7T vs. 4T: RF power, homogeneity, and signal-to-noise comparison in head images. *Magn Reson Med*. 2001;46:24–30.
16. Gruetter R, Weisdorf SA, Rajanayagan V, et al. Resolution improvements inin vivo1h NMR spectra with increased magnetic field strength. *J Magn Reson*. 1998;135:260–264.
17. Webb AG, Collins CM. Parallel transmit and receive technology in high-field magnetic resonance neuroimaging. *Int J Imaging Syst Technol*. 2010;20:2–13.
18. Collins CM, Liu W, Schreiber W, Yang QX, Smith MB. Central brightening due to constructive interference with,

without, and despite dielectric resonance. *J Magn Reson Imaging* 2005;21:192–196.

19. Hayes C, Edelstein W, Schenck J, Mueller O, Eash M. An efficient, highly homogeneous radiofrequency coil for whole-body NMR imaging at 1.5T. *J Magn Reson*. 1985;63:622–628.
20. Wiggins GC, Potthast A, Triantafyllou C, Wiggins CJ, Wald LL. Eight-channel phased array coil and detunable tem volume coil for 7T brain imaging. *Magn Reson Med*. 2005;54:235–240.
21. Vaughan J, Adriany G, Garwood M, et al. Detunable transverse electromagnetic (TEM) volume coil for high-field NMR. *Magn Reson Med*. 2002;47:990–1000.
22. Mekle R, van der Zwaag W, Joosten A, Gruetter R. Comparison of three commercially available radio frequency coils for human brain imaging at 3 tesla. *Magn Reson Mater Phys Biol Med*. 2008;21:53–61.
23. Potthast A, Wiggins G, Kraff O, et al. A 32 channel receive-only head coil and detunable transmit birdcage coil for 7 tesla brain imaging. In: Proceedings of the 14th Annual Meeting of ISMRM, Seattle, USA, 2006. Abstract 415.
24. Ledden P, Mareyam A, Wang S, van Gelderen P, Duyn J. 32 channel receive-only sense array for brain imaging at 7T. In: Proceedings of the 15th Annual Meeting of ISMRM, Berlin, Germany, 2007. Abstract 242.
25. Ipek O. Radio-frequency coils for ultra-high field magnetic resonance. *Analy Biochem*. 2017;529:10–16. Introduction to in vivo Magnetic Resonance Spectroscopy (MRS): a method to non-invasively study metabolism.
26. Katscher U, Börnert P, Leussler C, van den Brink JS. Transmit SENSE. *Magn Reson Med*. 2003;49:144–150.
27. Metzger GJ, Snyder C, Akgun C, Vaughan T, Ugurbil K, Van de Moortele PF. Local B_1^+ shimming for prostate imaging with transceiver arrays at 7T based on subject-dependent transmit phase measurements. *Magn Reson Med*. 2008;59:396–409.
28. Raaijmakers AJE, Ipek O, Klomp DWJ, et al. Design of a radiative surface coil array element at 7T: the single-side adapted dipole antenna. *Magn Reson Med*. 2011;66:1488–1497.
29. Ipek O, Raaijmakers A, Klomp D, Lagendijk J, Luijten P, Van den Berg C. Characterization of transceive surface elements designs for 7 tesla magnetic resonance imaging of the prostate: radiative antenna and microstrip. *Phys Med Biol*. 2012;57:343–355.
30. Ipek O, Raaijmakers A, Lagendijk J, Luijten P, van den Berg C. Optimization of the radiative antenna for 7-t magnetic resonance body imaging. *Concepts Magn Reson Part B*. 2013;43B: 1–10.
31. Oezerdem C, Winter L, Graessl A, et al. 16-channel bow tie antenna transceiver array for cardiac MR at 7.0 tesla. *Magn Reson Med*. 2016;75:2553–2565.
32. Steensma B, Obando A, Klomp D, Van den Berg N, Luijten P, Raaijmakers A. Body imaging at 7 tesla with much lower sar levels: an introduction of the snake antenna array. In: Proceedings of the 24th Annual Meeting of ISMRM, Singapore; 2016. Abstract 395.
33. Wiggins GC, Lakshmanan KChen G. The distributed inductance electric dipole antenna. In: Proceedings of the 23rd Annual Meeting of ISMRM, Toronto, Canada, 2015. Abstract 3100.
34. Ertürk MA, Raaijmakers AJE, Adriany G, Uğurbil K, Metzger GJ. A 16-channel combined loop-dipole transceiver array for 7 tesla body MRI. *Magn Reson Med*. 2017;77:884–894.
35. Chen G, Cloos M, Sodickson D, Wiggins G. A 7T 8 channel transmit-receive dipole array for head imaging: dipole element and coil evaluation. In: Proceedings of the 22nd Annual Meeting of ISMRM, Milan, Italy, 2014. Abstract 621.
36. Clément JD, Gruetter R, Ipek O. A human cerebral and cerebellar 8-channel transceive RF dipole coil array at 7T. *Magn Reson Med*. 2018;81:1447–1458.
37. Shajan G, Kozlov M, Hoffmann J, Turner R, Scheffler K, Pohmann R. A 16-channel dual-row transmit array in combination with a 31-element receive array for human brain imaging at 9.4 T. *Magn Reson Med*. 2014;71:870–879.
38. Adriany G, Auerbach EJ, Snyder CJ, et al. A 32-channel lattice transmission line array for parallel transmit and receive MRI at 7 tesla. *Magn Reson Med*. 2010;63:1478–1485.
39. Gilbert KM, Gati JS, Kho E, Klassen LM, Zeman P, Menon RS. An Parallel-Transmit, Parallel-Receive Coil for Routine Scanning on a 7T Head-Only Scanner. In: Proceedings of the 23rd Annual Meeting of ISMRM, Toronto, Canada; 2015. Abstract 623.
40. Avdievich N, Giapitzakis I, Pfrommer A, Borbath T, Henning A. Combination of surface and "vertical" loop elements improves receive performance of a human head transceiver array at 9.4 T. *NMR Biomed*. 2018;31:e3878. e3878 NBM-17-0089.R2.
41. Avdievich A, Giapitzakis I, Henning A. 32-channel combined surface loop/"vertical" loop tight-fit array provides for full-brain coverage, high transmit performance, and SNR improvement at 9.4t: an alternative to surface loop/dipole antenna combination. In: Proceedings of the 26th Annual Meeting of ISMRM, Paris, France, 2018. Abstract 140.
42. Ertürk MA, Raaijmakers AJ, Adriany G, Uğurbil K, Metzger GJ. A 16-channel combined loop-dipole transceiver array for 7 tesla body MRI. *Magn Reson Med*. 2017;77:884–894.
43. Steensma BR, Voogt IJ, Leiner T, et al. An 8-channel tx/rx dipole array combined with 16 RX loops for high-resolution functional cardiac imaging at 7T. *Magn Reson Mater Phys Biol Med*. 2018;31:7–18.
44. Qi D, Govind N, Natalia G, et al. A 7T spine array based on electric dipole transmitters. *Magn Reson Med*. 2015;74:1189–1197.
45. Dreyfuss H. *The Measure of Man: Human Factors in Design*. New York: Whitney Library of Design, 1969.
46. Gosselin M, Neufeld E, Moser H. Development of a new generation of high-resolution anatomical models for medical device evaluation: the virtual population 3.0. *Phys Med Biol*. 2014;59:5287.
47. Ipek O, Raaijmakers AJ, Lagendijk JJ, Luijten PR, van den Berg CAT. Intersubject local SAR variation for 7T prostate MR imaging with an eight-channel single-side adapted dipole antenna array. *Magn Reson Med*. 2014;71:1559–1567.
48. Kennedy J, Eberhart RC. Particle swarm optimization. In: Proceedings of the 1995 IEEE International Conference on Neural Networks, Perth, Australia, IEEE Service Center, Piscataway, NJ; 1995:1942–1948.
49. Clement J, Gruetter R, Ipek O. Comparison of passive RF phase shimming methods on the human brain at 7T using particle-swarm optimization. In: Proceedings of the 33rd Annual Meeting of ESMRMB, Vienna, Austria, 2016. Abstract 503.
50. Kellman P, McVeigh ER. Image reconstruction in SNR units: a general method for SNR measurement. *Magn Reson Med*. 2007;54:1439–1447.
51. Eggenschwiler F, Kober T, Magill AW, Gruetter R, Marques JP. Sa2rage: a new sequence for fast B_1^+-mapping. *Magn Reson Med*. 2012;67:1609–1619.
52. Marques JP, Kober T, Krueger G, van der Zwaag W, de Moortele PFV, Gruetter R. Mp2rage, a self bias-field corrected sequence for

improved segmentation and T_1-mapping at high field. *NeuroImage* 2010;49:1271–1281.
53. Keil B, Sappo C, Bilgic B, et al. Sub-millimeter cortical imaging at 7T using a high-density motor-cortex 32-channel array coil. In: Proceedings of the 25th Annual Meeting of ISMRM, Hawaï, USA, 2017. Abstract 1224.
54. Zhao W, Keil B, Polimeni J, et al. 16-channel TX array and 32-channel RX array for brain MRI at 7T. In: Proceedings of the 21st Annual Meeting of ISMRM, Salt Lake City, USA, 2013. Abstract 2724.
55. Gilbert KM, Gati JS, Barker K, Everling S, Menon RS. Optimized parallel transmit and receive radiofrequency coil for ultrahigh-field MRI of monkeys. *NeuroImage* 2016;125:153–161.
56. Lattanzi R, Wiggins GC, Zhang B, Duan Q, Brown R, Sodickson DK. Approaching ultimate intrinsic signal-to-noise ratio with loop and dipole antennas. *Magn Reson Med*. 2017;79:1789–1803.
57. Gras V, Vignaud A, Amadon A, Bihan D, Boulant N. Universal pulses: a new concept for calibration-free parallel transmission. *Magn Reson Med*. 2017;77:635–643.
58. Cloos MA, Boulant N, Luong M, et al. kT-points: short three-dimensional tailored RF pulses for flip-angle homogenization over an extended volume. *Magn Reson Med*. 2012;67:72–80.
59. Eggenschwiler F, O'Brien KR, Gruetter R, Marques JP. Improving T_2-weighted imaging at high field through the use of kT-points. *Magn Reson Med*. 2014;71:1478–1488.
60. Malik Shaihan J, Keihaninejad S, Hammers A, Hajnal JV. Tailored Excitation in 3D with Spiral Nonselective (SPINS) RF Pulses. *Magn Reson Med*. 2012;67:1303–1315.

SUPPORTING INFORMATION

Additional supporting information may be found online in the Supporting Information section at the end of the article.

FIGURE S1 A, Experimentally measured B_1^+ maps shown in the 3 orientations, and normalized to a 90° flip angle at the center of the brain for the in-house built 8Tx/32Rx coil array (upper row) and the commercial 1Tx/32Rx coil (bottom row). The total input voltages were 249V for the in-house built 8Tx/32Rx coil array and 187V for the commercial 1Tx/32Rx coil. For the in-house built 8Tx/32Rx coil array, the RF phases were optimized in transverse slice to cover the whole-brain. The same subject is shown for both coils. Nevertheless, the different fitting of the commercial 1Tx/32Rx coil on the head is responsible for the apparent differences on head's shape in sagittal slice. All measurements were performed within the SAR limits. B, Structural MP2RAGE image (0.6 mm-iso) masked to the brain tissues, and indicating the slices' positions shown in A, (white solid lines). The axial slice was oblique and oriented from the frontal to the occipital lobes

VIDEO S1 Animated high-resolution (0.6 mm-iso) sagittal slices acquired with the MP2RAGE sequence, and showing the whole-brain for the in-house built 8Tx/32Rx coil array. RF phases were optimized in transverse slice to cover the whole-brain

How to cite this article: Clément J, Gruetter R, Ipek Ö. A combined 32-channel receive-loops/8-channel transmit-dipoles coil array for whole-brain MR imaging at 7T. *Magn Reson Med*. 2019;00:1–13. https://doi.org/10.1002/mrm.27808